

**THE HETEROGENATION OF SACCHARIN,
MELAMINE AND SULFONIC ACID ONTO RICE HUSK
ASH SILICA AND THEIR CATALYTIC ACTIVITY IN
ESTERIFICATION REACTION**

KASIM MOHAMMED HELLO

UNIVERSITI SAINS MALAYSIA

2010

**THE HETEROGENATION OF SACCHARIN, MELAMINE AND
SULFONIC ACID ONTO RICE HUSK ASH SILICA AND THEIR
CATALYTIC ACTIVITY IN ESTERIFICATION REACTION**

by

KASIM MOHAMMED HELLO

**Thesis submitted in fulfilment of the requirements
for the degree of
Doctor of philosophy**

UNIVERSITI SAINS MALAYSIA

December 2010

ACKNOWLEDGEMENTS

I am grateful to University Sains Malaysia for the Ru grant (1001/PKIMIA/ 811092), Ru grant (1001/PKIMIA/814019), E-Science grant (305/PKIMIA/613317) and USM-RU-PRGS grant (1001/PKIMIA/842020). Thanks for Al-Muthanna University (Republic of Iraq) and all others who have rendered assistance and support in one way or another to make this study possible.

I would like to thank my supervisor Professor Farook Adam, for his continuous support during my Ph.D. research. He was always there to listen and to give advice. He taught me how to express my ideas. He showed me different ways to approach a research problem and the need to be persistent to accomplish any goal. I am also greatly indebted to my co-supervisor, Associated Professor Dr. Hasnah Osman for her support throughout the research period.

My gratitude also goes to the staff of the Schools of Chemistry, Biology and Physics of the University Sains Malaysia for their help in the necessary equipments. I also thank the NMR Research Center, IISc, Bangalore, India for recording the solid state NMR spectra.

I would like to thank Prof. Dr. Daniel Brunel (Mate'riaux Avance's pour la Catalyse et la Sante', Ecole Nationale Supe'rieure de Chimie, Montpellier, France) for critical discussions on the mechanism of the catalysis.

There is a long list of people who provided help. The list must start with Ali Jawad, Ghayth Al-Shaibani, Wisam, Ahmmed Hassan, Tamar, Alaa, Muslim, Assad, Bassam, Jassim, Iumu-Salmah, Hyder, Mohammed Talaq, Danial, Hanany, Muna, Ayad Mohammed (Babel University) and Jawad Al-Burke who gave me confidence and support.

Thanks also goes to my colleague, Dr. Adil Elhag Ahmed, Dr. T. Radhika, Dr. Mohd Aslam A.Pankhi, Dr. Imtiaz A. Khan (Post Doctoral Fellows), Shelly, Ishraqa, for helping solve unsolvable problems. Special thanks for my special friend Mohammed Anwar.

Special thanks are also due to my wife, Azhar, my three children, Mohammed, Nor Al-Hassan and Mohammed Ali, whose endless support and understanding have been profound throughout the difficult times.

TABLE OF CONTENTS

Acknowledgements.....	ii
Table of Contents.....	iii
List of Table.....	xii
List of Figures.....	xiv
List of Schemes.....	xxii
List of Appendixes.....	xxiv
List of Symbols and Abbreviation.....	xxvii
Abstrak.....	xxix
Abstract.....	xxxii

CHAPTER 1 – INTRODUCTION

1.0	Overview.....	1
1.1	Silica Modification.....	2
1.1.1	Immobilized Halide Systems.....	4
1.1.2	Immobilized Amine Ligand Systems.....	5
1.1.3	Immobilized Thiol Ligand Systems.....	6
1.2	Sol–Gel Process.....	7
1.3	Proposed Mechanism of Silica Gel Modified With Silylating Agent.....	9
1.4	Rice Husk.....	10
1.5	The Application of Silica From Rice Husk Ash (RHA).....	12
1.6	Saccharine.....	12
1.7	Melamine.....	14

1.8	Esterification.....	15
1.8.1	Esterification by Using Base Catalyst.....	17
1.8.2	Esterification by Using Acid Catalyst.....	20
1.9	Esterification of Long–Alkyl Chain Fatty Acid.....	21
1.10	Objectives of The Study.....	22
1.11	Outline of Thesis	23

CHAPTER 2 – EXPERIMENTAL METHODS

2.0	Raw Materials.....	25
2.1	Extraction of Silica From Rice Husk.....	25
2.2	Functionalization of RHA With CPTES.....	26
2.3	Functionalization of RHA With APTES and MPTMS.....	27
2.4	Catalyst Preparation.....	27
2.4.1	Preparation of Solid Sac Catalyst, RHAC-Sac.....	27
2.4.2	Preparation of Solid Mela Catalyst, RHAPrMela.....	27
2.4.3	Preparation of Solid Sulfonic Acid Catalyst, RHAPrSO ₃ H.....	28
2.5	Physico–Chemical Characterization.....	28
2.5.1	Elemental Analysis.....	29
2.5.2	Nitrogen Adsorption Analysis.....	29
2.5.3	Thermogravimetric analysis (TGA)/Differential thermal analysis (DTA).....	29
2.5.4	X–Ray Diffraction (XRD).....	30
2.5.5	Fourier Transform Infra–Red Spectroscopy (FT-IR).....	30
2.5.6	²⁹ Si MAS NMR Spectroscopy.....	30
2.5.7	¹³ C CP/MAS NMR Spectroscopy.....	31

2.5.8	Scanning Electron Microscopy–Energy Dispersive X–ray (SEM/EDX).....	31
2.5.9	Transmission Electron Microscopy (TEM).....	32
2.5.10	Cation Exchange Capacity CEC.....	32
2.5.11	Pyridine acidity test.....	32
2.6	Catalytic Reactions.....	33
2.6.1	Reaction Procedures.....	33
2.6.2	The Optimisation of The Mass of Catalyst.....	33
2.6.3	The Optimisation of The Reactants Mole Ratio.....	34
2.6.4	The Optimisation of The Reaction Temperatures	34
2.6.5	The Reusability of The Catalysts.....	34
2.6.6	Reaction Procedures For Homogenous Catalysts.....	34
2.6.7	Analysis By Gas Chromatography and Mass Spectroscopy (GC and GC–MS).....	35

CHAPTER 3– THE SYNTHESIS AND CHARACTERIZATION OF RHA SILICA MODIFIED WITH SILYATING AGENTS

3.0	Introduction.....	36
3.1	The Synthesis and Characterization of RHACCl.....	40
3.1.1	Elemental Analysis.....	40
3.1.2	The Nitrogen Adsorption Analysis.....	41
3.1.3	Thermogravimetric Analysis (TGA)/Differential Thermal Analysis (DTA).....	43
3.1.4	The Determination of Percentage Loading of Organic Ligands.....	45

3.1.5	Powder X-ray Diffraction (XRD).....	46
3.1.6	Fourier Transformed Infrared Spectroscopy Analysis (FT-IR).....	47
3.1.7	Solid-State MAS NMR.....	48
3.1.7.1	The ^{29}Si MAS NMR.....	48
3.1.7.2	The ^{13}C CP/MAS NMR.....	50
3.1.8	Electron Micrographs (SEM and TEM).....	51
3.2	The Synthesis and Characterization of RHAPrNH ₂	53
3.2.1	Elemental Analysis.....	54
3.2.2	The Nitrogen Adsorption Analysis.....	54
3.2.3	Thermogravimetric analysis (TGA)/Differential thermal analysis (DTA).....	55
3.2.4	The Determination of Percentage Loading of Organic Ligands.....	56
3.2.5	Powder X-ray Diffraction (XRD).....	57
3.2.6	Fourier Transformed Infrared Spectroscopy Analysis (FT-IR).....	57
3.2.7	Solid-State MAS NMR.....	59
3.2.7.1	The ^{29}Si MAS NMR.....	59
3.2.7.2	The ^{13}C CP/MAS NMR.....	61
3.2.8	Electron Micrographs (SEM and TEM).....	61
3.3	The Synthesis and Characterization of RHAPrSH.....	62
3.3.1	Elemental Analysis.....	63
3.3.2	The Nitrogen Adsorption Analysis.....	64
3.3.3	Thermogravimetric analysis (TGA)/Differential thermal analysis (DTA).....	65
3.3.4	The Determination of Percentage Loading of Organic Ligands.....	67

3.3.5	Powder X-ray Diffraction (XRD).....	67
3.3.6	Fourier Transformed Infrared Spectroscopy Analysis (FT-IR).....	67
3.3.7	Solid-State MAS NMR.....	69
3.3.7.1	The ²⁹ Si MAS NMR.....	69
3.3.7.2	The ¹³ C CP/MAS NMR.....	70
3.3.8	Electron Micrographs (SEM and TEM).....	71
3.4	Conclusions.....	71

CHAPTER 4– THE SYNTHESIS AND CHARACTERIZATION OF HETEROGENEOUS SACCHARINE, MELAMINE AND SULFONIC ACID

4.0	Introduction.....	73
4.1	The Synthesis and Characterization of Solid Sac catalyst, RHAC-Sac.....	73
4.1.1	Elemental Analysis.....	74
4.1.2	The Nitrogen Adsorption Analysis.....	75
4.1.3	Thermogravimetric analysis (TGA)/Differential thermal analysis (DTA).....	76
4.1.4	Powder X-ray Diffraction (XRD).....	77
4.1.5	Fourier Transformed Infrared Spectroscopy Analysis (FT-IR).....	78
4.1.6	Solid-State MAS NMR.....	80
4.1.6.1	The ²⁹ Si MAS NMR.....	80
4.1.6.2	The ¹³ C CP/MAS NMR.....	81
4.1.7	Electron Micrographs (SEM and TEM).....	83
4.2	The Synthesis and Characterization of Solid Melamine Catalyst, RHAPrMela.....	84

4.2.1	Elemental Analysis.....	84
4.2.2	The Nitrogen Adsorption Analysis.....	85
4.2.3	Thermogravimetric analysis (TGA)/Differential thermal analysis (DTA).....	87
4.2.4	The Determination of Percentage Loading of Organic Ligands.....	88
4.2.5	Powder X-ray Diffraction (XRD).....	88
4.2.6	Fourier Transformed Infrared Spectroscopy Analysis (FT-IR).....	89
4.2.7	Solid-State MAS NMR.....	90
4.2.7.1	The ^{29}Si MAS NMR.....	90
4.2.7.2	The ^{13}C CP/MAS NMR.....	92
4.2.8	Electron Micrographs (SEM and TEM).....	93
4.3	The Synthesis and Characterization of solid sulfonic acid catalyst, RHAPrSO ₃ H.....	95
4.3.1	Elemental Analysis.....	96
4.3.2	The Nitrogen Adsorption Analysis.....	97
4.3.3	Thermogravimetric analysis (TGA)/Differential thermal analysis (DTA).....	99
4.3.4	Powder X-ray Diffraction (XRD).....	100
4.3.5	Fourier Transformed Infrared Spectroscopy Analysis (FT-IR).....	101
4.3.6	Solid-State MAS NMR.....	102
4.3.6.1	The ^{29}Si MAS NMR.....	102
4.3.6.2	The ^{13}C CP/MAS NMR.....	104
4.3.7	Electron Micrographs (SEM and TEM).....	104
4.3.8	Cation Exchange Capacity (CEC).....	106

4.3.9	The Surface Acidity.....	106
4.4	Conclusions.....	107
CHAPTER 5– ESTERIFICATION STUDIES		
5.0	Introduction.....	109
5.1	Catalytic Study With RHAC-Sac Catalyst.....	109
5.1.1	Influence of Reaction Time.....	109
5.1.2	Effect of Catalyst Mass.....	110
5.1.3	Influence of Molar Ratio of The Reactants.....	111
5.1.4	Influence of Reaction Temperature.....	112
5.1.5	Reusability Studies of RHAC-Sac.....	113
5.1.6	The Esterification of Higher Alcohols With Acetic Acid Over RHAC-Sac.....	114
5.1.7	The Esterification of Other Acids With Methanol Over RHAC-Sac.....	115
5.1.8	Reaction Kinetics.....	117
5.1.9	The Possible Mechanism of Esterification Assisted by The Lactam Ring.....	119
5.2	Catalytic Study Over RHAPrMela Catalyst.....	120
5.2.1	Influence of Reaction Time.....	121

5.2.2	Effect of Catalyst Mass.....	122
5.2.3	Influence of Molar Ratio of The Reactants.....	123
5.2.4	Influence of Reaction Temperature.....	124
5.2.5	Reusability Studies of RHAPrMela.....	124
5.2.6	Esterification of Higher Alcohols With Acetic Acid Over RHAPrMela.....	125
5.2.7	Esterification of Higher Acids With Methanol Over RHAPrMela.....	126
5.2.8	Reaction Kinetics.....	127
5.2.9	The Proposed Mechanism.....	129
5.3	Catalytic Esterification with RHAPrSO ₃ H.....	130
5.3.1	Influence of Reaction Time.....	131
5.3.2	Effect of Catalyst Mass.....	132
5.3.3	Influence of Molar Ratio of The Reactants.....	133
5.3.4	Influence of Reaction Temperature.....	134
5.3.5	The Catalyst Reusability of RHAPrSO ₃ H.....	135
5.3.6	The Esterification of Higher Alcohols With Acetic Acid Over RHAPrSO ₃ H.....	137
5.3.7	Esterification of Other Acids With Methanol Over RHAPrSO ₃ H...	137

5.3.8	Reaction Kinetics.....	139
5.3.9	The Proposed Mechanism.....	140
5.4	Conclusions.....	142

CHAPTER 6 – CONCLUSIONS & RECOMMENDATIONS

6.0	Conclusion.....	144
6.1	Comparison Between Catalysts Loading.....	145
6.2	Comparison Between Catalysts Activity.....	146
6.3	The Equilibrium Time of RHAC-Sac, RHAPrMela and RHAPrSO ₃ H.....	152
6.4	The Water Poisoning.....	153
6.5	The Reaction Mechanisms.....	153
6.6	The Homogeneous and The Blank Catalysts.....	154
6.7	Recommendations.....	155
	References.....	156
	Appendixes.....	169
	List of Publications.....	206
	List of Conferences.....	207

LIST OF TABLES

	Page	
Table 1.1	Chemical composition of RHA after burning out at 700 °C for 6 h	11
Table 3.1	Literature review of the techniques used to immobilize silica with different silylating agents and the application of these hybrids	37
Table 3.2	The chemical analysis of RHA and RHACCl using a combination of elemental and EDX analysis	41
Table 3.3	The result of BET analysis for RHA and RHACCl	43
Table 3.4	The physical parameters obtained for RHAPrNH ₂ . The C, H and N content determined by a combination of elemental and EDX analysis. The value for oxygen has been omitted. The result of BET analysis are also shown	54
Table 3.5	The physical parameters obtained for RHAPrSH. The C, H and N content determined by combination of elemental and EDX (average of two areas and one spot) analysis. The value for oxygen has been omitted. The results of BET analysis are also shown	64
Table 4.1	The physical parameters obtained for RHAC-Sac. The C, H and N content determined by combination of elemental and EDX analysis. The average values obtained from EDX analysis for RHAC-Sac. The value for oxygen has been omitted. The result of BET analysis was also shown	75
Table 4.2	The physical parameters obtained for RHAPrMela. The C, H and N content determined by combination of elemental and EDX analysis. The average values obtained from EDX analysis for RHAPrMela. The value for oxygen has been omitted	85
Table 4.3	The physical parameters obtained for RHAPrSO ₃ H. The percentage of elements content determined by combination of elemental and EDX analysis. The average values obtained from EDX analysis for RHAPrSO ₃ H	97
Table 5.1	The kinetic parameters for the conversion of ethyl alcohol over the surface of RHAC-Sac. k_a is the apparent rate constant, E_a activation energy and A frequency factor	119
Table 5.2	The kinetic parameters for the conversion of ethyl alcohol over the surface of RHAPrMela. k_a is the apparent rate constant, E_a activation energy and A frequency factor	129

Table 5.3	The kinetic parameters for the conversion of ethyl alcohol over the surface of RHAPrSO ₃ H. k_a is the apparent rate constant, E_a activation energy and A frequency factor	140
Table 6.1	Percentage of peak areas of ²⁹ Si MAS NMR of RHAC-Sac, RHAPrMela and RHAPrSO ₃ H and percentage of loading of organic ligands	146
Table 6.2	TON and TOF values calculated for different heterogeneous and homogeneous catalysts catalyzed esterification of ethanol with acetic acid at 85 °C with 1:1 mole ratio	168
Table 6.3	A summary of the catalysts used in the esterification reaction as compared with RHAC-Sac, RHAPrMela and RHASO ₃ H	150

LIST OF FIGURES

		Page
Fig. 1.1	Types of silanol groups and siloxane bridges on the surface of silica	2
Fig.1.2	The dimerization of two molecules of Sac via H–bonds giving rise to the eight member ring structure	14
Fig. 1.3	Some examples of base functionalized silica. (a) piperidine, (b) 1,5,7–triazabicyclo[4.4.0]dec–5–ene, (c) (1 <i>R</i> ,2 <i>S</i>)–ephedrine	18
Fig.1.4	The relative catalytic activity of various organic molecules in the acylation reaction	18
Fig. 3.1	The nitrogen adsorption–desorption isotherm of RHACCl. The inset shows the corresponding pore size distribution	42
Fig. 3.2	Thermogravimetric analysis (TGA)/differential thermal analysis (DTA) of (a) RHA, (b) RHACCl.	44
Fig: 3.3	The X–ray diffraction pattern for RHACCl shows typical amorphous	47
Fig. 3.4	The FT-IR spectra of RHA, RHACCl and the differential spectrum	48
Fig. 3.5	The silica surface with silicon atoms of various bridging bonds T ^{<i>m</i>} sites (<i>m</i> = 1, 2 or 3)	49
Fig. 3.6	The ²⁹ Si MAS NMR solid–state spectra of (a) RHA and (b) RHACCl	49
Fig. 3.7	The possible structures for RHACCl as suggested by MAS NMR and FT-IR. (a) T ³ – Three siloxane bonds to silicon. (b) T ² – two siloxane bonds to silicon. It also shows C1, C2 and C3 as identified in the solid state ¹³ C CP/MAS NMR spectrum	50
Fig. 3.8	The solid–sate ¹³ C CP/MAS NMR spectra for RHACCl shows three peaks C1, C2, and C3 of the incorporated chloropropyl group	51
Fig. 3.9	The SEM image of RHACCl ca. (a) at 3 K magnification, (b) at 300 K magnification	52
Fig. 3.10	The TEM image of RHACCl. (a, b) at 450 K magnification	52

Fig. 3.11	The nitrogen adsorption–desorption isotherms of RHAPrNH ₂ . The inset shows the corresponding pore size distribution which was highly irregular	55
Fig. 3.12	Thermogravimetric analysis (TGA)/differential thermal analysis (DTA) for RHAPrNH ₂ . Three characteristic decomposition stages are shown.	56
Fig. 3.13	The X–ray diffraction pattern for RHAPrNH ₂ which shows typical amorphous	57
Fig. 3.14	The FT-IR spectra of RHA, RHAPrNH ₂ and the differential spectrum	58
Fig. 3.15	The solid–stat ²⁹ Si MAS NMR of RHAPrNH ₂ . The chemical shifts of T ¹ , T ² , T ³ , Q ² , Q ³ and Q ⁴ are observed	59
Fig. 3.16	The possible structures for RHAPrNH ₂ as suggested by MAS NMR and FT-IR. (a) T ³ – three siloxane bonded to silicon. (b) T ² – two siloxane bonded to silicon. (c) T ¹ – one siloxane bonded to silicon	60
Fig. 3.17	The solid–stat ¹³ C CP/MAS NMR spectra of RHAPrNH ₂ shows three peaks C1, C2, and C3 of the incorporated aminopropyl group onto RHA	61
Fig. 3.18	The SEM micrographs of RHAPrNH ₂ at different magnification: (a) at 5 K magnification, (b) at 30 K magnification	62
Fig. 3.19	The nitrogen adsorption–desorption isotherms of RHAPrSH. The inset shows the corresponding pore size distribution	65
Fig. 3.20	Thermogravimetric analysis (TGA)/differential thermal analysis (DTA) for RHAPrSH. Three characteristic decomposition stages are shown.	66
Fig. 3.21	The X–ray diffraction pattern for RHAPrSH which shows typical amorphous	67
Fig. 3.22	The FT-IR spectra of RHA, RHAPrSH and the differential spectrum	68
Fig. 3.23	The solid–stat ²⁹ Si MAS NMR spectra of RHAPrSH. The chemical shifts of T ¹ , T ² , T ³ , Q ² , Q ³ and Q ⁴ are observed	69
Fig. 3.24	The solid–stat ¹³ C CP/MAS NMR spectra of RHAPrSH. The C2 and C3 signals were superimposed on each other	70

Fig. 3.25	The SEM micrographs of RHAPrSH at different magnification ca. (a) at 5 K magnification, (b) at 40 K magnification	71
Fig. 4.1	The nitrogen adsorption/desorption isotherms of RHAC-Sac. The inset shows the corresponding pore size distribution	76
Fig. 4.2	Thermogravimetric analysis (TGA)/differential thermal analysis (DTA) for RHAC-Sac. Three characteristic decomposition stages are shown	77
Fig. 4.3	The X-ray diffraction pattern shows amorphous nature of RHAC-Sac	78
Fig. 4.4	The FT-IR spectra of RHACCl, RHAC-Sac and the differential	79
Fig. 4.5	The ^{29}Si MAS NMR solid-state spectrum of RHAC-Sac. The chemical shifts of T^2 , T^3 , Q^3 and Q^4 are observed	81
Fig. 4.6	The possible structures for RHAC-Sac as suggested by MAS NMR and FT-IR. (a) T^3 – three siloxane bonded to silicon. (b) T^2 – two siloxane bonded to silicon	81
Fig. 4.7	The solid-state ^{13}C CP/MAS NMR spectra for RHAC-Sac. The carbon of Sac and propyl group are shown	82
Fig. 4.8	The SEM images of RHAC-Sac at ca. (a) 4 K magnification, (b) 30 K magnification, showing the irregular pore arrangements	83
Fig. 4.9	The TEM images of RHAC-Sac at 450 K magnification showing the irregular pores arrangements.	83
Fig. 4.10	(a) The nitrogen adsorption/desorption isotherms of RHAPrMela. (b) The corresponding pore size distribution	86
Fig. 4.11	Thermogravimetric analysis (TGA)/differential thermal analysis (DTA) for RHAPrMela. For characteristic decomposition stages are shown	88
Fig. 4.12	The X-ray diffraction pattern shows amorphous nature of RHAPrMela	89
Fig. 4.13	The FT-IR spectra of RHACCl, RHAPrMela and the differential spectra	90
Fig. 4.14	The ^{29}Si MAS NMR solid-state spectrum of RHAPrMela. The chemical shifts of T^2 , T^3 , Q^3 and Q^4 are observed	91

Fig. 4.15	The possible structures for RHAPrMela as suggested by MAS NMR and FT-IR. (a) T ³ – three siloxane bonds to silicon. (b) T ² –two siloxane bonds to silicon	91
Fig. 4.16	The solid–state ¹³ C CP/MAS NMR spectra for RHAPrMela (a) at 7 KHz and (b) at 5 KHz. It also shows C1, C2, C3, C4 and C5 (two carbon atoms are labeled as C5 due to their similar chemical environment). The spinning side bands marked *	93
Fig. 4.17	The SEM micrographs of RHAPrMela at different magnifications (a) at 5.5 K magnification, (b) at 11.0 K magnification. (c, d) at 1.1 K magnification (e) at 60 K magnification	94
Fig. 4.18	The TEM images of RHAPrMela, (a) at 26 K magnification, (b) at 85 K magnification (c) at 70 K magnification (d) at 140 K magnification	95
Fig. 4.19	The nitrogen adsorption/desorption isotherms of RHAPrSO ₃ H. The inset shows the corresponding pore size distribution	98
Fig. 4.20	Thermogravimetric analysis (TGA)/differential thermal analysis (DTA) for RHAPrSO ₃ H. Three characteristic decomposition stages are shown	100
Fig. 4.21	The X–ray diffraction pattern shows amorphous nature of RHAPrSO ₃ H	101
Fig. 4.22	The FT-IR spectra of RHAPrSH, RHAPrSO ₃ H and the differential	102
Fig. 4.23	The solid–stat ²⁹ Si MAS NMR of RHAPrSO ₃ H. The T ² and T ¹ signals can be seen after 5 times magnifying the area between 40 to 60 ppm	103
Fig. 4.24	The possible structure for RHAPrSO ₃ H as suggested by MAS NMR and FT-IR. (a) T ³ – three siloxane bonded to silicon. (b) T ² – two siloxane bonded to silicon. (c) T ¹ – one siloxane bonded to silicon. The carbons of the propyl chain (C1, C2 and C3) were identified by their ¹³ C CP/MAS NMR spectrum	103
Fig. 4.25	The solid–state ¹³ C CP/MAS NMR spectra for RHAPrSO ₃ H shows three peaks C1, C2, and C3 of the incorporated propyl group onto RHAPrSO ₃ H	104
Fig. 4.26	The SEM micrograph of RHAPrSO ₃ H at ca. 17.5 K magnification	105

Fig. 4.27	The TEM image of RHAPrSO ₃ H, (a, b) at 140 K magnification and (c, d) at 280 K magnification. Regular and spherical shaped particles were obtained	105
Fig. 4.28	The FT-IR spectra of RHAPrSO ₃ H in absorption mode. (a) Before pyridine adsorption, (b) after pyridine adsorption	107
Fig. 5.1	The conversion of ethyl alcohol in the esterification of ethyl alcohol with acetic acid over RHAC-Sac (heterogeneous) and homogeneous saccharine as a function of reaction time. The reaction conditions were: catalyst 0.1g, Sac 1.87 mg (0.0102 mol), mole ratio of acid: alcohol = 1:1 and reaction temperature (85 °C).	110
Fig. 5.2	The conversion of ethyl alcohol in the esterification of ethyl alcohol with acetic acid over RHAC-Sac as a function of mass of catalyst. The reaction conditions were: mole ratio of acid: alcohol =1:1, 6 h reaction time at 85 °C	111
Fig. 5.3	The conversion of ethyl alcohol in the esterification of ethyl alcohol with acetic acid over RHAC-Sac with different molar ratios of acid to alcohol and alcohol to acid. The reaction conditions were: catalyst 0.10 g, at 85 °C and 6 h reaction time	112
Fig. 5.4	The conversion of ethyl alcohol in the esterification of ethyl alcohol with acetic acid over RHAC-Sac at different temperatures. The reaction conditions were: catalyst 0.1 g, mole ratio of acid: alcohol = 1:1 and 6 h reaction time	113
Fig. 5.5	The reusability of RHAC-Sac in the esterification of ethyl alcohol with acetic acid. (a) Catalyst regenerated by washing with alcohol and heating at 110 °C for 24 h. (b) Catalyst regenerated by washing with alcohol and heating at 150 °C for 24 h. The reaction conditions were: catalyst 0.1 g, mole ratio of acid: alcohol = 1:1, at 85 °C and reaction time 6 h	114
Fig. 5.6	The conversion of alcohol in the esterification reaction over RHAC-Sac. The reaction conditions were: catalyst 0.1 g, mole ratio of acid: alcohol =1:1, reaction temperature 85 °C and reaction time 6 h. PrOH = 1-propanol, 2-PrOH= 2-propanol, t-BuOH = tert-butanol, BuOH = butanol, and BzOH = benzyl alcohol	115
Fig. 5.7	The conversion of methanol in the esterification reaction over RHAC-Sac. The reaction conditions were: catalyst 0.1 g, reaction temperature 75 °C and reaction time 6 h. Acetic acid (C2), capric acid (C10) and myristic acid (C14)	116

Fig. 5.8	The second order rate plots for the conversion of ethyl alcohol over the surface of RHAC-Sac at different temperatures. The reaction conditions were: catalyst 0.1 g, mole ratio of acid: alcohol =1:1 and 6 h reaction time	117
Fig. 5.9	Pseudo Arrhenius plot for the conversion of ethyl alcohol over the surface of RHAC-Sac at different temperatures. The reaction conditions were: catalyst 0.1 g, mole ratio of acid: alcohol =1:1 and 6 h reaction time	118
Fig. 5.10	Conversion of ethyl alcohol in the esterification of ethyl alcohol with acetic acid over RHAPrMela and homogenous Mela as a function of reaction time. Reaction condition: catalyst 0.1 g (RHAPrMela) and 0.0088 g (Mela), mole ratio of reactant acid: alcohol =1:1 at 85 °C	121
Fig. 5.11	The conversion of ethyl alcohol in the esterification of ethyl alcohol with acetic acid over RHAPrMela as a function of the mass of catalyst. The reaction conditions were: mole ratio of acid: alcohol = 1:1, 9 h reaction time and 85 °C as a reaction temperature	122
Fig. 5.12	The conversion of ethyl alcohol with acetic acid over RHAPrMela with different molar ratio of acid to alcohol and alcohol to acid. The reaction conditions were: catalyst 0.10 g, at 85 °C and 9 h reaction time	123
Fig. 5.13	The conversion of ethyl alcohol with acetic acid over RHAPrMela at different temperatures. The reaction conditions were: catalyst 0.1 g, mole ratio of acid: alcohol = 1:1 and 9 h reaction time	124
Fig. 5.14	The reusability of RHAPrMela in the esterification of ethyl alcohol with acetic acid. The reaction conditions were: catalyst 0.1 g, mole ratio of acid: alcohol = 1:1, at 85 °C and 9 h reaction time. The regeneration temperature was 150 °C	125
Fig. 5.15	The conversion of alcohol in the esterification reaction over RHAPrMela. The reaction conditions were: catalyst 0.1 g, mole ratio of acid: alcohol =1:1, at 85 °C and 9 h reaction time. PrOH = 1-propanol, 2-PrOH = 2-propanol, t-BuOH = tert-butanol, BuOH = butanol, and BzOH = benzylalcohol	126
Fig. 5.16	The conversion of methanol in the esterification reaction over RHAPrMela. The reaction conditions were: catalyst 0.1 g, reaction temperature 75 °C and reaction time 9 h. Acetic acid (C2), capric acid (C10) and myristic acid (C14)	127

Fig. 5.17	The pseudo second order rate plots for the conversion of ethyl alcohol over the surface of RHAPrMela at different temperatures. The reaction conditions were: catalyst 0.1 g, mole ratio of acid: alcohol = 1:1 and 9 h reaction time	128
Fig. 5.18	Pseudo Arrhenius plot for the conversion of ethyl alcohol over the surface of RHAPrMela at different temperatures. The reaction conditions were: catalyst 0.1 g, mole ratio of acid: alcohol 1:1 and 9 h reaction time	128
Fig. 5.19	The catalytic esterification of ethyl alcohol with acetic acid over RHAPrSO ₃ H and RHA–Blank as a function of reaction time. The reaction conditions were: 0.1 g catalyst mass, mole ratio of acid: alcohol = 1:1 and reaction temperature 85 °C	132
Fig. 5.20	The catalytic esterification of ethyl alcohol with acetic acid over RHAPrSO ₃ H as a function of catalyst mass. The reaction conditions were: 0.1 g catalyst mass, mole ratio of acid: alcohol = 1:1 and reaction temperature 85 °C	133
Fig. 5.21	The conversion of ethyl alcohol over RHAPrSO ₃ H with different molar ratio of acid to alcohol and alcohol to acid. The reaction conditions were: 0.1 g catalyst mass, reaction temperature 85 °C and reaction time 8 h	134
Fig. 5.22	The conversion of ethyl alcohol with acetic acid over RHAPrSO ₃ H at different temperatures. The reaction conditions were: 0.1 g catalyst mass, mole ratio of acid: alcohol = 1:1 and reaction time 8 h	135
Fig. 5.23	The regeneration and catalytic reusability of RHAPrSO ₃ H in the esterification reaction. (a) The effect of regeneration temperature and percentage conversion of ethanol, (b) the reusability of RHAPrSO ₃ H without loss of catalytic efficiency, after regeneration at 185 °C. Reaction condition: 0.1 g catalyst mass, 85 °C reaction temperature, mole ratio of acid: alcohol = 1:1 and 8 h reaction time	136
Fig. 5.24	The conversion of alcohol in the esterification reaction over RHAPrSO ₃ H. The reaction conditions were: catalyst 0.1 g, mole ratio of acid: alcohol = 1:1, reaction temperature 85 °C and reaction time 8 h.	137
Fig. 5.25	The conversion of methanol in the esterification reaction over RHAPrSO ₃ H. The reaction conditions were: 0.1 g of the catalyst, reaction temperature is 75 °C and 8 h as a reaction time. Acetic acid (C2), capric acid (C10) and myristic acid (C14)	138

Fig. 5.26	The second order rate plots for the conversion of ethyl alcohol over the surface of RHAPrSO ₃ H. The reaction condition: catalyst 0.1 g, mole ratio of acid: alcohol = 1:1 and 8 h reaction time at different temperature. The correlation coefficients were also shown	139
Fig. 5.27	Pseudo Arrhenius plot for the conversion of ethyl alcohol over the surface of RHAPrSO ₃ H at different temperatures. The reaction conditions were: catalyst 0.1 g, mole ratio of acid: alcohol = 1:1 and 8 h reaction time	140
Fig. 6.1	The structure of (a) RHAPrMela, (b) guanidine and (c) melamine. The aromatic ring in (a) and (c) can be derived from assembling the guanidine molecule in (b)	147
Fig. 6.2	The comparative plot of the catalytic esterification of ethyl alcohol with acetic acid over RHAPrSO ₃ H, RHAC-Sac and RHAPrMela as a function of reaction time. The reaction conditions were: 0.1 g catalyst mass, mole ratio of acid:alcohol = 1:1 and reaction temperature 85 °C	152
Fig. 6.3	The proposed eight member ring transition state formed by the hydrogen bonding as a result of adsorbed reactants on the catalysts. (a) RHAC-Sac, (b) RHAPrMela and (c) RHAPrSO ₃ H	154

LIST OF SCHEMES

	Page	
Scheme 1.1	(a) The reaction of silylating agent with the ligand complex followed by immobilizes the resulting ligand onto silica. (b) The immobilized of silylating agent onto silica followed by immobilized the ligand complex.	4
Scheme 1.2	The usual steps of a sol–gel process	8
Scheme 1.3	The probable reaction during the hydrolysis of alcohol and water condensation in the sol–gel processes	9
Scheme 1.4	The reaction mechanism for the condensation of silylating agent onto silica.	10
Scheme 1.5	The reaction of alcohol with organic acid to produce ester	15
Scheme 3.1	The reaction sequence and the possible structures for RHACCl, as suggested by MAS NMR and FT-IR. (a) T ³ – attributed to the silicon atom of the CPTES forming three siloxane bonds with the silicon of the RHA. (b) T ² – is assigned to the formation of two siloxane bonds with the silicon of RHA and one OH group bonded to the silicon atom of the CPTES	40
Scheme 3.2	The reaction sequence and the possible structures for RHAPrNH ₂ as suggested by MAS NMR and FT-IR. a) T ³ – attributed to the silicon atom of the APTES forming three siloxane bonds with the silicon of the RHA. (b) T ² – is assigned to the formation of two siloxane bonds with the silicon of RHA and one OH group bonded to the silicon atom of the APTES. (c) T ¹ – is assigned to the formation of one siloxane bonds with the silicon of RHA and two OH group bonded to the silicon atom of the APTES	53
Scheme 3.3	The reaction sequence and the possible structures for RHAPrSH as suggested by MAS NMR and FT-IR. a) T ³ – attributed to the silicon atom of the MPTMS forming three siloxane bonds with the silicon of the RHA. (b) T ² – is assigned to the formation of two siloxane bonds with the silicon of RHA and one OH group bonded to the silicon atom of the MPTMS. (c) T ¹ – is assigned to the formation of one siloxane bonds with the silicon of RHA and two OH group bonded to the silicon atom of the MPTMS	63

Scheme 4.1	The reaction Scheme for the immobilization of Sac onto RHACCl to form RHAC-Sac. (a) T^3 – three siloxane bonds to silicon. (b) T^2 – two siloxane bonds to silicon. It also shows C1, C2 and C3 as identified in the solid– state ^{13}C CP/MAS NMR spectrum. The approximate time taken for the completion of the experimental process is also shown	74
Scheme 4.2	The reaction sequence and the possible structures for RHAPrMela as suggested by MAS NMR and FT-IR. (a) T^3 – Three siloxane bonds to silicon. (b) T^2 – two siloxane bonds to silicon. It also shows C1, C2, C3,C4 and C5 (two carbon atoms are labeled as C5 due to their similar chemical environment) as identified in the solid–state ^{13}C CP/MAS NMR spectrum. The approximate times taken for the completion of the experimental processes are also shown	84
Scheme 4.3	The reaction sequence for the synthesis of RHAPrSO ₃ H. The possible structures of the catalyst are represented from MAS NMR and FT-IR spectra studies. (a) T^3 –three siloxane bonds to silicon. (b) T^2 –two siloxane bonds to silicon. (c) T^1 –one siloxane bonds to silicon. The carbons of the propyl chain (C1, C2 and C3) were identified by their ^{13}C CP/MAS NMR spectrum	96
Scheme 5.1	A suggested reaction mechanism for the esterification of alcohol with acetic acid on the RHAC-Sac surface	120
Scheme 5.2	The involvement of the nitrogen centers on the melamine in the reaction mechanism for the esterification of ethyl alcohol with acetic acid on the surface of RHAPrMela. The fixation of the acid on the catalyst is via the formation a stable eight member ring transition structure	130
Scheme 5.3	The suggested catalytic cycle for the esterification reaction with RHAPrSO ₃ H as the catalyst. (a) The ion pair carbocation	141

LIST OF APPENDIXES

Appendix A–Fourier Transformed Infrared FT-IR		Page
A1	The FT-IR spectra of the evolved gasses of RHAC-Sac	169
A2	The FT-IR spectrum of the evolved gasses of RHAC-Sac shows the physical H ₂ O matching with the library spectra	169
A3	The FT-IR spectrum of the evolved gasses of RHAC-Sac shows the liberation of CH ₃ NO matching with the library spectra	170
A4	The FT-IR spectrum of the evolved gasses of RHAC-Sac shows the liberation of SO ₂ matching with the library spectra	170
A5	The FT-IR spectrum of the evolved gasses of RHAPrMela shows the liberation of C, H and N matching with the library spectra	171
A6	The FT-IR spectrum of the evolved gasses of RHAPrMela shows the liberation of H ₂ O, C ₄ H ₉ N and C ₂ H ₃ matching with the library spectra	171
A7	The FT-IR spectrum of the evolved gasses of RHAPrMela shows the liberation of H ₂ O and C ₇ H ₇ N matching with the library spectra.	172
A8	The FT-IR spectrum of the evolved gasses of RHAPrMela shows the liberation of H ₂ O, C ₂ H ₃ and C ₄ H ₉ NO matching with the library spectra	172
A9	The FT-IR spectrum of the evolved gasses of RHAPrMela shows the liberation of H ₂ O, C ₆ H ₅ and CHN matching with the library spectra	173
A10	The FT-IR spectrum of the evolved gasses of RHAPrMela shows the liberation of H ₂ O and C ₂ H ₃ matching with the library spectra	173
A11	The FT-IR spectrum of the evolved gasses of RHAPrMela shows the liberation of H ₂ O and C ₂ H ₃ matching with the library spectra	174
A12	The FT-IR spectrum of the evolved gasses of RHAPrMela shows the liberation of CO, C ₃ H ₅ NO and C ₇ H ₅ NO matching with the library spectra	174

A13	The FT-IR spectrum of the evolved gasses of RHAPrMela shows the liberation of H ₂ O, CO ₂ and C ₂ H ₃ matching with the library spectra	175
A14	The FT-IR spectra of RHAC-Sac. The fresh catalyst and after first re-used	175
A15	The FT-IR spectra of RHAPrMela. The fresh catalyst and after first re-used	176
A16	The FT-IR spectra of RHAPrSO ₃ H. The fresh catalyst and after first re-used	176

Appendix B– Transmission Electron Microscopy (TEM)

B1	The TEM image of RHAPrNH ₂ at ca. 240 K magnification	177
B2	The TEM image of RHAPrSH, (a) at ca.190 K magnification and (b) at ca. 300 K magnification	177

Appendix C– Gas chromatography (GC)

C1	Gas chromatography (GC) chromatogram for conversion of ethyl alcohol with acetic acid over RHAPrSO ₃ H at different time. (a) At 0 h, (b) 3 h and (c) at 8 h. The reaction conditions were: catalyst used 0.1 g, mole ratio of acid: alcohol = 1:1	179
C2	GC–MS data for conversion of ethyl alcohol with acetic acid.	180
C3	GC–MS data for conversion of propyl alcohol with acetic acid	182
C4	GC–MS data for conversion of butyl alcohol with acetic acid	184
C5	GC–MS data for conversion of 2–propyl alcohol with acetic acid	186
C6	GC–MS data for conversion of ter–butyl alcohol with acetic acid	188
C7	GC–MS data for conversion of benzyl alcohol with acetic acid	190
C8	GC–MS data for conversion of myristic acid (C14) with methanol	193
C9	GC–MS data for conversion of capric acid (C10) with methanol	197
C10	GC–MS data for conversion of acetic acid (C2) with methanol	199

Appendix D– Energy Dispersive X–ray (EDX)

Fig. D1	The one area, table of element continent and EDX spectra of RHACCI	200
Fig. D2	The one spot, table of element continent and EDX spectra of RHAPrNH ₂	201
Fig. D3	The one spot, table of element continent and EDX spectra of RHAPrSH	202
Fig. D4	The one spot, table of element continent and EDX spectra of RHAC-Sac	203
Fig. D5	The one spot, table of element continent and EDX spectra of RHAPrMela	204
Fig. D6	The one spot, table of element continent and EDX spectra of RHAPrSO ₃ H	205

LIST OF SYMBOLS AND ABBREVIATIONS

APTES	3-(aminopropyl)triethoxysilane
AR	Room Temperature
CHN	Carbon, Hydrogen, and Nitrogen Elemental Analysis
ca.	Calculated
CP	Cross Polarisation
CPTES	3-(chloropropyl)triethoxysilane
DMF	Di-methylformamide
DCM	Di-chloromethane
E_a	Activation Energy
EDX	Energy Dispersive X-ray
Fig	Figure
FT-IR	Fourier Transform Infra-Red spectroscopy
Et_3N	Tri-ethylamine
GC	Gas Chromatography
GC-MS	Gas Chromatography Mass Spectroscopy
IUPAC	The International Union of Pure and Applied Chemistry
R	Alkyl group
RHA	Rice husk ash
MPTMS	3-(mercaptopropyl)trimethoxysilane
N	Surface Coverage
Sac	Saccharine
SEM	Scanning Electron Microscopy

Si–OH	Silanol
Si–O–Si	Siloxane
k_a	The Apparent Rate Constant
kJ	Kilo joule (The unit of energy)
M	Molar Amount of Grafted
Mela	Melamine
MAS NMR	Magic angle–spinning Nuclear Magnetic Resonance
pp	Page
P/P_o	Relative Pressure
pH	The Hydrogen Function
P_w	Weight Percentage
T	Tesla (Unit For Measuring Magnetic Induction)
TEM	Transmission Electron Microscopy
TGA	Thermogravimetric Analyses
XRD	X–ray Diffraction

PENGHETEROGENAN SAKARINA, MELAMINA DAN ASID SULFONIK KE ATAS SILIKA ABU SEKAM PADI DAN AKTIVITI PEMANGKINAN DI DALAM TINDAK BALAS PENGESTERAN

ABSTRAK

Natrium silikat daripada abu sekam padi (RHA) telah dimodifikasikan dengan 3-(kloropropil)trietoksisilan (CPTES), 3-(merkaptopropil)trimetoksisilan (MPTMS) dan 3-(aminopropil)trietoksisilan (APTES) untuk menghasilkan RHACCl, RHAPrSH dan RHAPrNH₂ melalui kaedah sintesis one-pot. Analisis ²⁹Si MAS NMR pada RHACCl menunjukkan kewujudan pusat silikon T², T³, Q³ dan Q⁴ manakala pusat silikon T¹, T², T³, Q², Q³ dan Q⁴ wujud pada RHAPrSH dan RHAPrNH. Spektrum ¹³C MAS NMR menunjukkan RHACCl mempunyai 3 anjakan kimia pada 10.37, 26.70 dan 47.69 ppm yang merujuk kepada 3 atom karbon moiti CPTES. RHAPrSH mempunyai anjakan kimia pada 16.59, 32.73 dan 14.58 manakala RHAPrNH₂ menunjukkan hanya dua daripada tiga jalur yang dijangkakan pada 26.13 dan 47.87 ppm disebabkan oleh pertindihan kedua jalur antara satu sama lain. Kombinasi analisis CHN dan EDX telah menunjukkan kewujudan unsur klorin di dalam RHACCl, sulfur di dalam RHAPrSH, nitrogen di dalam RHAPrNH₂ dan seterusnya kewujudan karbon dan silikon yang membuktikan silylating agents bergabung dengan silika RHA. Sakarin (Sac) dan Melamina (Mel) immobilized dengan silika untuk membentek RHAC-Sac dan RHAPrMela. Kedua spektrum ²⁹Si MAS NMR, RHAC-Sac dan RHAPrMela menunjukkan anjakan kimia yang sama dengan RHACCl. Spektrum ¹³C MAS NMR menunjukan RHAC-Sac mempunyai siri anjakan kimia yang konsisten dengan kehadiran gelang aromatik dan laktam. Dua anjakan kimia pada 161.52 dan 169.67 ppm dengan jalur sisi putaran dubel pada ¹³C MAS NMR RHAPrMela, menunjukkan tiga atom karbon di dalam gelang

melamina tidak ekuivalen dalam RHAPrMela. Kumpulan berfungsi $-\text{CH}_2-\text{SH}$ dalam RHAPrSH telah dioksidakan ke asid sulfonik, $-\text{CH}_2-\text{SO}_3\text{H}$ dengan hidrogen peroksida pada suhu bilik. ^{29}Si MAS NMR menunjukkan anjakan kimia yang serupa dengan RHAPrSH. Tiada pertindihan anjakan kimia C3 dan C2 dalam ^{13}C MAS NMR diperhatikan selepas transformasi kepada RHAPrSO₃H. RHAC-Sac, RHAPrMela, RHAPrSO₃H dan RHA-Blank (kawalan) berserta dengan Sac dan Mela homogen digunakan sebagai mangkin dalam tindak balas esterifikasi. Aktiviti mangkin keatas ester didapati mengikut urutan berikut:

RHAPrSO₃H > RHAPrMela > Sac homogen > RHAC-Sac > Mela homogen > RHA-Blank.

Mangkin diaktifkan semula dengan pemanasan untuk mengeluarkan air dan boleh digunakan semula beberapa kali tanpa kehilangan sifat mangkinnya.

THE HETEROGENATION OF SACCHARIN, MELAMINE AND SULFONIC ACID ONTO RICE HUSK ASH SILICA AND THEIR CATALYTIC ACTIVITY IN ESTERIFICATION REACTION

ABSTRACT

Sodium silicate from rice husk ash (RHA) was functionalized with 3-(chloropropyl)triethoxysilane (CPTES), 3-(mercaptopropyl)trimethoxysilane and 3-(aminopropyl)triethoxysilane to give RHACCl, RHAPrSH and RHAPrNH₂ via a simple one-pot synthesis. The ²⁹Si MAS NMR of RHACCl showed the presence of T², T³, Q³ and Q⁴ silicon centres, while the T¹, T², T³, Q², Q³ and Q⁴ silicon centres were present in both RHAPrSH and RHAPrNH₂. The ¹³C MAS NMR showed that RHACCl had three chemical shifts at 10.37, 26.70 and 47.69 ppm, which was attributed to the three carbon atoms of the CPTES moiety. RHAPrNH₂ had chemical shifts at 16.59, 32.73 and 14.58, while RHAPrSH showed only two signals at 26.13 and 47.87 ppm instead of the expected three signals. This was due to the superimposition of two signals on each other. The combination of elemental and EDX analysis showed the presence of chlorine in RHACCl, sulfur was found in RHAPrSH and nitrogen was found in RHAPrNH₂ as well as the presence of carbon and silicon in the samples confirmed that the silylating agents were incorporated onto RHA silica. Saccharine (Sac) and Melamine (Mela) were immobilized onto RHACCl to form RHAC-Sac and RHAPrMela. Both ²⁹Si MAS NMR spectra of RHAC-Sac and RHAPrMela showed similar chemical shifts to the RHACCl. The ¹³C MAS NMR showed that RHAC-Sac had a series of chemical shifts consistent with the presence of the aromatic and lactam ring. Two chemical shifts at 161.52 and 169.67 ppm with double spinning side bands were seen in the ¹³C MAS NMR of RHAPrMela, indicating that the three carbon atoms in the melamine ring were not

equivalent. The functionalized $-\text{CH}_2\text{-SH}$ group in RHAPrSH was oxidized to sulfonic acid, $-\text{CH}_2\text{-SO}_3\text{H}$ with hydrogen peroxide at room temperature. The ^{29}Si MAS NMR showed similar chemical shifts to the RHAPrSH. No overlapping of the C3 and C2 chemical shifts in the ^{13}C MAS NMR was observed after the transformation to RHAPrSO₃H. RHAC-Sac, RHAPrMela, RHAPrSO₃H, RHA-Blank (as control) as well as homogenous Sac and homogenous Mela were used as catalysts in the esterification reaction. The catalytic activity of the catalysts toward the respective esters was found to follow the sequence below.

RHAPrSO₃H > RHAPrMela > homogenous Sac > RHAC-Sac > homogenous Mela > RHA-Blank.

The catalysts were easily regenerated by heating to remove water and could be reused several times without loss of catalytic activity.

Chapter One

Introduction

1.0 Overview

Zhuravlev (2000) and Vansant, et al. (1995) stated that studies on silica started in the 1930s when a number of scholars such as Endell, Wilm, Carman and Rideal studied the condensation processes of silicic acids which led to the discovery of surface silanol groups, $\equiv\text{Si}-\text{OH}$. After that, by using an infrared spectroscopy method, Yaroslavsky and Terenin had proved the presence of hydroxyl groups on the silica surface (porous glass) (Zhuravlev, 2000). Because of numerous spectral and chemical data, it has become well known that silica has two types of functional groups, i.e. the siloxane ($\equiv\text{Si}-\text{O}-\text{Si}\equiv$) in the bulk and several forms of silanol groups ($\equiv\text{Si}-\text{OH}$) on its surface.

There are two surface silanol groups found experimentally on the silica surface: the isolated (a single hydroxyl group attached to the silicon atom, $\equiv\text{SiOH}$) and the geminal (two hydroxyls group attached to the same silicon atom, $=\text{Si}(\text{OH})_2$) as shown in Fig 1.1. Hydrogen bonds can be formed between the two vicinal silanol groups (Yang, et al., 2006). On the other hand, silica shows three types of siloxane groups ($\equiv\text{Si}-\text{O}-\text{Si}\equiv$). According to NMR study, these siloxane groups ($\equiv\text{Si}-\text{O}-\text{Si}\equiv$) are represented as Q^n , where n indicates the number of bridging bonds ($-\text{O}-\text{Si}$) tied to the central Si atom, i.e.: Q^4 – four siloxane bonds to the silicon atom; Q^3 – three siloxane bonds to the silicon atom; and Q^2 – two siloxane bonds to the silicon atom

as shown in Fig 1.1. Generally, the number of siloxane groups can be determined from the following equation: $Q^n = \text{Si} (\text{OSi})_n(\text{OH})_{4-n}$ (Zhang, et al., 2006).

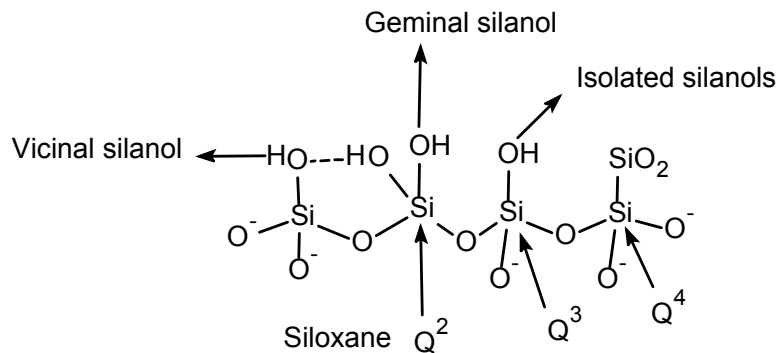


Fig. 1.1: Types of silanol groups and siloxane bridges on the surface of silica [adopted from Zhuravlev, 2000].

1.1 Silica Modification

The modification of the silica surface has received a great deal of attention (Brunel, 1999; Bae, et al., 2000; Airoidi & Arakaki, 2001; Al-Nahhal, et al., 2007; Gübbük, et al., 2008). This process can empower the researchers to control and change the chemical properties and technological characteristics of the composite material. The modification of the silica surface is important for the preparation of essential for the synthesis of materials with many specific properties; these could be for the preparation of selective heterogeneous catalysts, nanostructured silica materials and liquid crystals (Tertykh & Belyakova, 1996).

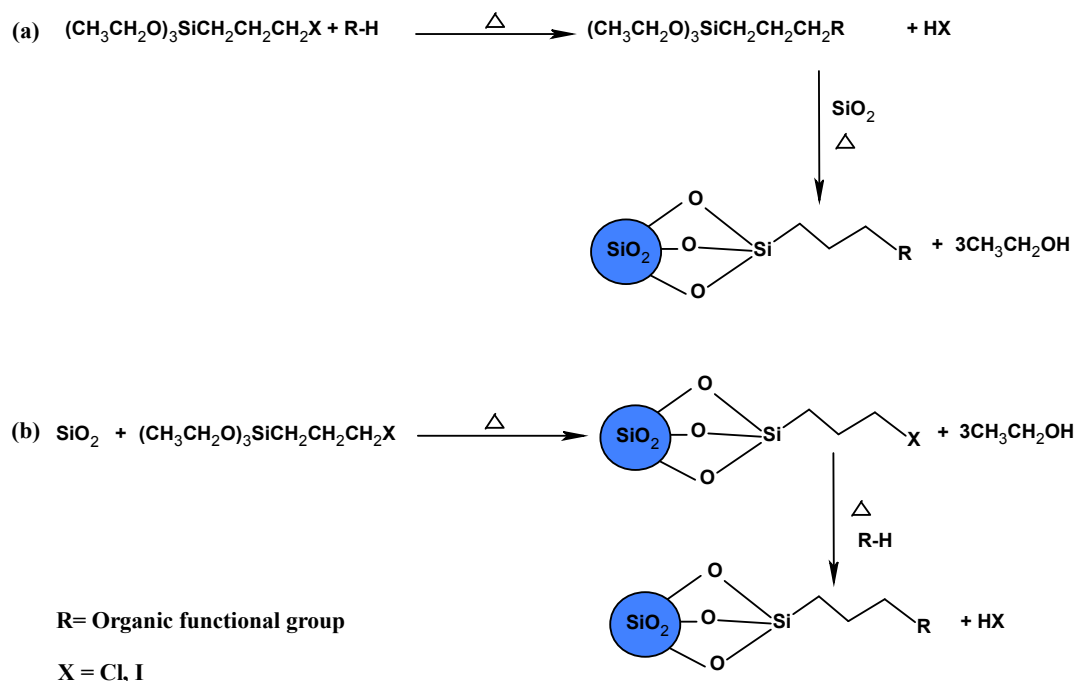
The silanol groups on the silica surface play a significant role during modification of the surface with alkyl silanes (Dash, et al., 2008). As the temperature increases, the silanol groups on the silica surface are dehydrated. The continuous

increase in temperature leads to the dehydration of silanol groups (Peng, et al., 2009) resulting in the formation of siloxane bond.

The modification of silica is mostly carried out by using organic molecules in order to functionalize its surface. Silylating agents are chemically reactive towards the free silanol groups on the silica surface (Cestari, et al., 2001). The silylating agents are usually alkoxy silanes with general formula $(RO)_3Si-R^*$, where R is methyl or ethyl groups and R^* is an n -propylic carbon chain containing an end functional groups, e.g.: amine, halogen or sulfur group, or a combination of them (Cestari & Airoidi, 1997).

Silica modified with silylating agent is one of the best choices to introduce basic groups through an anchored pendant chain (Prado & Airoidi, 2001a). One of the important advantages of the immobilization of functional groups on silica via this route is to make the organic functional group resistant to removal from the surface by different organic solvent or water (Arakaki & Airoidi, 2000). It also offers good thermal and hydrolytic stability with accessibility to the reactive centres (Prado & Airoidi, 2001b; Filha, et al., 2006).

There are two strategies for the immobilization of the silylating agents. The first strategy is to react the silylating agents with the ligand complex, and then to immobilize the resulting ligand with the pre-formed silica in a heterogeneous reaction as in Scheme 1a. The second strategy is to treat the post-polysiloxane with the complex group as in Scheme 1b.



Scheme 1.1: (a) The reaction of silylating agent with the ligand complex followed by immobilizes the resulting ligand onto silica. (b) The immobilized of silylating agent onto silica followed by immobilized the ligand complex.

Both strategies have been studied widely by many researchers (Vrancken, et al., 1995; Brunel, 1999; Bae, et al., 2000; Hoegaerts, et al., 2000; Airoidi & Arakaki, 2001; Al-Nahhal, et al., 2007; El-Ashgar, et al., 2007; Gübbük, et al., 2008; Shi & Wei, 2008). It was observed that these two reported preparation methods involved long preparation times and they utilized hazardous chemicals leading to inefficient preparation techniques as discussed in the sub-section below.

1.1.1 Immobilized halide systems

Silica modified with 3-(chloropropyl)triethoxysilane (CPTES) is usually carried out in a solid-liquid mixed phase reaction (heterogeneous reaction). Bae, et al. (2000), Hoegaerts, et al. (2000), Shi and Wei (2008) had reported that the reaction needs to be refluxed in toluene for 12–24 h. This is followed by soxhlet extraction

with different organic solvents such as toluene and dichloromethane. Brunel (1999) had reported the functionalization of silica (which was pre-dried at 150 °C at 10⁻¹ Torr for 12 h) by refluxing it with CPTES in toluene at 120 °C with total time of approximately 14 h. Alcântara, et al. (2007) showed that 3-(chloropropyl)triethoxysilane (CPTMS) can also be used to functionalize silica to produce the same product. However, the reaction needs to be refluxed for 72 h at 150 °C. The same reaction was carried out by Soundiressane, et al. (2007) by refluxing CPTMS with silica for 24 h, followed by soxhlet extraction with dichloromethane (DCM) for 12 h. Kovalchuk, et al. (2006) had reported that amorphous silica needs to be refluxed in aqueous HNO₃ (2 M) for 6–10 h, followed by washing with distilled water and dried at 150 °C for 4 h. Finally, the post-synthetic treatment was performed to graft the silica with CPTES, by heating at 130–150 °C in air or at 200 °C under vacuum.

1.1.2 Immobilized amine ligand systems

The condition for functionalization of 3-(aminopropyl)triethoxysilane (APTES) is almost similar to CPTES. Hoegaerts, et al. (2000) took 31 h, using toluene, diethyl ether and dichloromethane as solvents during various stages of the transformation. While Macquarrie and Jackson (1997) and Macquarrie (1996) took 21 h to functionalize APTMS onto silica, employing different techniques such as reflux and extraction. Brunel (1999) also needed 27 h to fabricate APTES onto silica. However, the temperature used was quite high, i.e. 120 °C and 150 °C for the fabrication reaction. Brunel used toluene, diethyl ether and DCM as solvents during the reaction and the extraction procedures. Wu, et al. (2008) had reported the functionalization of silica by refluxing it with APTES in toluene, followed by soxhlet extraction with total time of approximately 48 h. The method used by

Vejayakumaran, et al. (2008) needed 36 h to fabricate APTES onto silica. Multiple technique, higher temperature and different organic solvents were used during these fabrication process.

1.1.3 Immobilized thiol ligand systems

Silica gel modified with 3-(trimethoxysilyl)propane-1-thiol (MPTMS) has been studied by Eunice, et al. (1997) and Simoni, et al. (2000). Functionalized polysiloxane containing thiol ligand was prepared by hydrolytic polycondensation of silica with $(\text{MeO})_3\text{Si}(\text{CH}_2)_3\text{SH}$. The anchored thiol groups can be oxidized to provide sulfonic acid functionality for the applications in solid acid catalysts (Yang, et al., 2005). The potential use of these derivatives as well as other organo functional derivatives critically depends on the loading of accessible functional groups into the framework (Prado & Arakaki, 2001c).

To graft MPTMS onto silica, Yang, et al. (2005) took 5 days to immobilize it onto silica using different hazardous organic solvents. Shylesh, et al. (2004) modified the silica with MPTMS in 61 h, and used toluene and methanol during the process under a nitrogen atmosphere. The method used by Bossaert, et al. (1999) needed 54 h to fabricate MPTMS onto silica. They used multiple techniques and different organic solvents during the fabrication process. Karimi and Khalkhali (2005) and Gupta, et al. (2007) had tried to activate the silica by refluxing in concentrated hydrochloric acid for 24 h; and then they proceeded with another reflux with MPTMS in dry toluene for 18 h. They also used soxhlet extraction for 36 h. The total time required for the whole process was 78 h.

The brief review above shows that the present methods to functionalize silica with CPTES, APTES and MPTMS resulted in low yield, employing harsh reaction conditions, multiple steps, long reaction time, using non-environmental friendly organic solvents, use of high energy, and costly chemicals. Therefore, there is a need to design a new method which is easy, cost-effective, environment-friendly, time saving, minimal energy loss, high yield and can be used especially in the heterogenation of homogeneous catalysts. Such a method could have a wide impact.

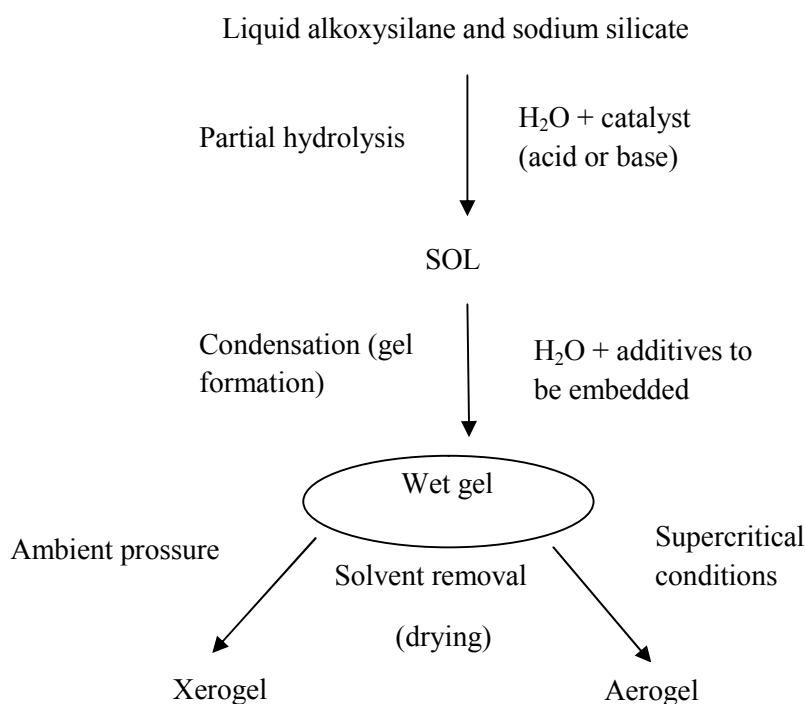
1.2 Sol-gel process

Sol-gel method is one of the well known wet chemical methods. It is a transitional process between a liquid phase “sol” to the solid phase “gel” (Ahmed, 2008); or it can be seen as a hydrolysis and condensation of silicon (or any other metal alkoxides) and organoalkoxysilanes (Hofacker, et al., 2002).

The recent great interest in organic-inorganic hybrid materials prepared by sol-gel chemistry along with the growing interest in functionalization of inorganic matrices may be due to the ease in which it can be used to design unique materials with controllable pore size, structural rigidity, thermal stability, and enhanced recognition properties (Airoldi and Arakaki, 2001; Arrachart, et al., 2009).

According to Prokopowicz, et al. (1998), more than 89 % of the literature describing the application of materials to chemically modify surfaces deals with sol-gel. The sol-gel process comprises several steps in general. When the silicate precursor mixes with silylating agent in the presence of the solvent (water or alcohol) and a catalyst (acid or base), which was stirred for several hours, leads to

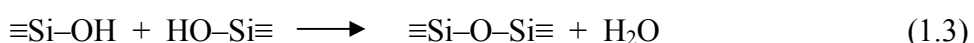
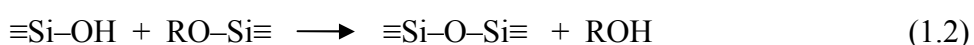
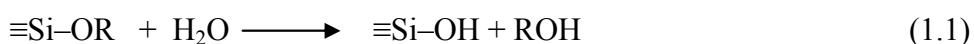
partial hydrolysis of the Si–O–R (R = methyl or ethyl group) bonds in the silylating agent. When alcohol is used as a solvent, the hydrogel structure will be formed. There are some parameters that control the hydrogel structure. These parameters include temperature, pH of the medium, nature of the solvent, nature of the added electrolyte and the type of the starting salt or alkoxide. The xerogel is formed by aging and drying the gel. If the gel has a very large pore volume (up to 98 % of the total volume), it is named as aerogel (Vansant, et al., 1995). Scheme 1.2 shows the details of these (Teoli, et al., 2006).



Scheme 1.2: The usual steps of a sol–gel process [adapted from Teoli, et al., (2006)].

Scheme 1.3 shows some equations of reaction proposed by Chen and Lin (2003). This is to explain the hydrolysis and polymerization which may take place in the sol–gel processes. As shown in the reaction equations below, hydrolysis of the

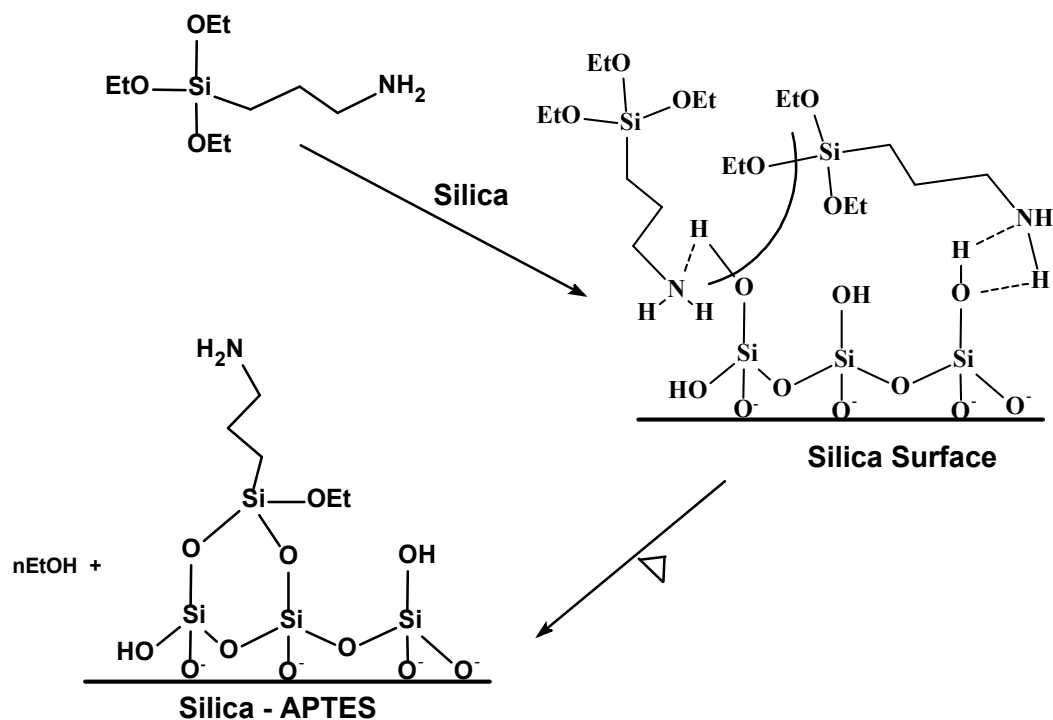
precursor produces a sol of soluble hydroxylated monomer (equation 1.1), followed by polymerization and phase separation to form a hydrated oxide hydrogel (equation 1.2). Controlled removal of water from the wet gel by extraction or drying produces the dry, porous xerogel (equation 1.3).



Scheme 1.3: The probable reaction during the hydrolysis of alcohol and water condensation in the sol-gel processes.

1.3 Proposed mechanism of silica gel modified with silylating agent

The reaction mechanism between silylating agent and silica gel could be a type of condensation reaction. The general sequence for the condensation of APTES is given in Scheme 1.4. In this type of mechanism, small molecules will be liberated as a result of the condensation. According to Vansant, et al. (1995), and Vrancken, et al. (1995) the initial step of silica modification includes physical adsorption. This physisorption depends on the availability of silanol groups on the silica surface and the hydrogen bond between silanol groups and the silylating agent. The hydrolysis of ethoxy silane group leads to form silanol group. The formed silanol group will be condensed to form siloxane bonds at the surface.



Scheme 1.4: The reaction mechanism for the condensation of silylating agent onto silica.

1.4 Rice Husk

Rice husk (RH) is a cellulose-based fibre which is suitable for recycling (Ndazi, et al., 2007). Rice is grown in over 75 countries (Huang, et al., 2001). The annual world rice production amounts to 400 – 545 million metric tons, of which more than 10 % is husk (Conradt, et al., 1992; Mansaray and Ghaly, 1998; Feng, et al., 2004). Due to the high silica content in the husk (Yalçın, et al., 2000), it makes economic sense to utilize this free raw material. RH contains about 20 % silica which can be extracted and used in many areas where commercial silica is being used (Della, et al., 2002).

Rice husk is composed of 20 % ash, 38 % cellulose, 22 % lignin, 18 % pentose, and 2 % other organic components and water (Adam & Chua, 2004). Burning the rice husk causes environmental pollution. Therefore, efforts have been

made to burn the husks under moderate temperature and pressure (Feng, et al., 2004). When burning the rice husk, a white ash which is porous silica with high specific surface area can be obtained (Watari, et al., 2006). This ash (RHA) contains more than 95 % silica. Table 1.1 below shows a typical analysis of RHA obtained at 700 °C (Della, et al., 2002). It can be seen that ca. 95 % of the ash is composed of silica, SiO₂.

Table 1.1: Chemical composition of RHA after burning out at 700 °C for 6 h [adapted from Della, et al., (2002)].

Oxides	Component expressed as RHA %
SiO ₂	94.95
Al ₂ O ₃	0.39
Fe ₂ O ₃	0.26
CaO	0.54
Na ₂ O	0.25
K ₂ O	0.94
MnO	0.16
TiO ₂	0.02
MgO	0.90
P ₂ O ₅	0.74
Loss on ignition at 700 °C	0.85

1.5 The applications of silica from rice husk ash (RHA)

The existence of silica in RHA was known since in 1938. The acid leaching, pyrolysis, and carbon-removing processes from rice husk can give amorphous silica (Radhika & Sugunan, 2006). The purity of silica in RHA can reach as high as 99.9 % (Chang, et al., 2003). The silica extracted from rice husk has many advantageous properties, such as high chemical and thermal stability, high specific surface area, high porosity, good accessibility (Gupta, et al., 2007), and functionalization of organic groups can be robustly anchored to the surface.

Chang, et al. (2003) was the first to describe the use of RHA as a support for heterogeneous catalyst. He used RHA as a support for nickel catalyst which exhibited a very high activity in the hydrogenation of CO₂. Adam, et al. (1990, 2004, 2006, 2007, and 2008) have described the use of RHA silica as a support for different metals, such as, Al, Gl, In, Fe, and Ru and used them as heterogeneous catalysts for different purposes.

1.6 Saccharine

Saccharine (Sac) or *o*-sulfobenzimide was discovered accidentally by Fahlberg in 1878 during his PhD research, and published it a year later (Remsen & Fahlberg, 1879). A short time after this discovery, Sac was produced on an industrial scale as the first sweetening agent which does not contain carbohydrate, with a sweetening power of about 550 times that of sucrose (Ellis, 1995; Baran, et al., 2006).

Sac can be synthesized by the oxidation of *o*-toluenesulfonamide using KMnO_4 in a base medium to produce sodium *o*-sulfonamidobenzoate which can give Sac by acidifying the latter, using HCl (Vogel, 1973).

Sac has different hetero atoms within its molecule, one N, one O (carbonylic) and two S=O (sulfonic) atoms. Using these donor atoms, the anion can generate either N- or O-monodentate or bidentate (N, O) coordination, and also more complex polymeric species with the participation of all possible donor atoms. These atoms have lone pair electrons which combine with the strained ring of the Sac molecule. This could in essence act as catalytic sites imparting a certain degree of selectivity. These hetero atoms can also be used to form coordination bonds with transition metals that can be utilized further for catalysis. In this regard, Adam, et al. (2007) had reported the synthesis of a Sac-Cu coordination complex, $\text{Cu}(\text{Sac})_2 \cdot 2\text{H}_2\text{O}$ which has a square planar configuration at the copper centre. It is believed that these complexes could be more useful if they were immobilized onto solids.

Several Sac derivatives were synthesized by Yablonsky, et al. (2001); they have found applications for the monomers of polycondensation, bioactive substances, and additives improving the nickel plating process and others. Their study also proved that Sac molecules can associate with carbonyl groups due to H-bonds and it can also form eight member ring dimers (see Fig. 1.2).

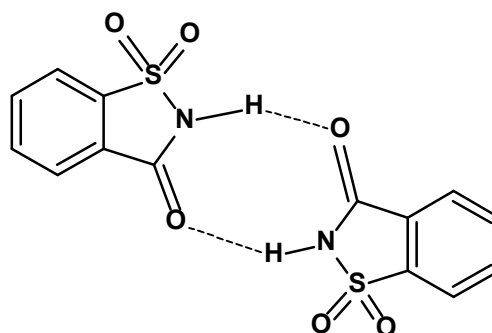


Fig. 1.2: The dimerization of two molecules of Sac via H-bonds giving rise to the eight member ring structure.

1.7 Melamine

Melamine (Mela) (1,3,5-triazine-2,4,6-triamine) with a chemical formula of $C_3H_6N_6$ is an organic compound that consists of 66 % nitrogen (Wu, et al., 2009). It has several industrial uses such as in the manufacture of amino resins and plastics (Cook, et al., 2005; Buu, et al., 2008).

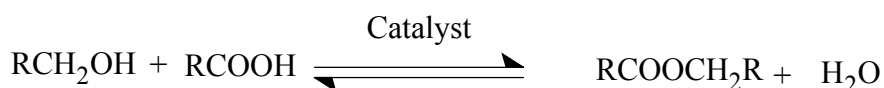
Mela was first synthesized by Justus von Liebig in 1834 by heating dicyandiamide above its melting temperature (Bozzi, et al., 2004). Mela is commercially available and it has been used in a wide range of products. For example, it is combined with formaldehyde to produce melamine resin as durable thermosetting plastic, and melamine foam as a polymeric cleaning product (Rima, et al., 2008). However, it must be acknowledged that the recent misuse of Mela in tainted infant milk powder raised awareness worldwide. It also raised our curiosity and interest due to the presence of a large number of heteroatoms in the Mela molecule.

Mela can directly react with reducing sugars (specifically with lactose and Strecker aldehydes) to consequently interfere with Maillard reactions in chemical

model systems. It was found that Mela influences the levels of different kinds of volatile products and colour development in Maillard¹ models. The presence of melamine in foods can therefore have a significant impact on various organoleptic properties (Ma, et al., 2010).

1.8 Esterification

The condensation of organic acids and alcohols produce esters, (see Scheme 1.5). The esters with small molecular weight are industrially important intermediate class of substances in the synthesis of fine chemicals, polyesters, drugs, plasticisers, food preservatives, pharmaceuticals, solvents (for cellulose, oils, gums, and resins), perfumes, cosmetics, pesticides and chiral auxiliaries (Haslam, 1980; Lilja, et al., 2002; Bhagiyalakshmi, et al., 2004; Palani & Pandurangan, 2005).



R = alkyl or aryl group

Scheme 1.5: The reaction of alcohol with organic acid to produce ester.

¹*Maillard reactions*: the reaction of active carbonyl group of the reducing sugars (such as glucose, fructose and lactose) with the nucleophilic amino groups of amino acids, peptides or proteins, and subsequently produces a large number of poorly characterised compounds, contributing to the colour and flavour of foods.

Esterification reaction is a liquid-phase process and can take place without adding catalysts due to the weak acidity of carboxylic acids. However, the reaction requires several days to attain equilibrium in the absence of catalysts (Liu, et al., 2006a). Therefore, adding a catalyst for the liquid-phase process is necessary (Ajaikumar & Pandurangan, 2007). There are two types of catalysts for the esterification reactions, either homogenous, by strong mineral acids or heterogeneous. The mineral acid used for the esterification reaction involves the use of H_2SO_4 , HCl , HF , H_3PO_4 and ClSO_2OH . These acids suffer from drawbacks such as high toxicity and corrosion. The excess acid has to be neutralized after the reaction and left behind considerable amounts of salts to be disposed off into the environment. Since all these substances are miscible with the reaction medium it is very difficult to separate them, and reusability of the catalyst is usually not possible (Lu, 1995; Liu & Tan, 2001; Harmer & Sun, 2001; Lilja, et al., 2002).

Hence, the catalyst for this process should be replaced by a heterogeneous process; therefore, there is a need to design a heterogeneous catalyst (Sheldon, 1997). The design of new heterogeneous catalysts requires some conditions. One of these conditions is the availability and simplicity of the preparation procedures. It must be also cost-effective, and reduce the waste to minimize environmental pollution which is a crucial factor for developing environmentally friendly catalysts. The recoverable and reusability is also one of the important conditions and advantages of heterogeneous catalysts (Liu & Tan, 2001; Harmer & Sun, 2001; Dash & Parida, 2007).

In this regard, several types of heterogeneous catalysts have been reported in the literature for esterification. These include iodine (Ramalinga, et al., 2002), copper (Inui, et al., 2002), lipase (Novak, et al., 2003), MCM-41 (Díaz, et al., 2001; Koster, et al., 2001), zeolites beta (da Silva-Machado, et al., 2000), ion exchange resin (Gimenez, et al., 1987), supported acids (Yang, et al., 2005), and acidic ionic liquids (Gui, et al., 2004). There are two types of heterogeneous catalysts for the esterification reaction, i.e. acid catalysts and base catalysts. Both catalysts are discussed in detail below.

1.8.1 Esterification by using base catalyst

Esterification by base catalysts has not received much attention because it is usual to use acids to catalyse this reaction. A reaction between a carbon-halogen functional group and an organic base or ligand such as amine groups is a nucleophilic substitution reaction (Cauvel, et al., 1997; Lasperas, et al., 1997). These organic amines and ammonium salts have been used as base heterogeneous catalysts for esterification reactions (Barcelo, et al., 1990; Gui, et al., 2004).

In this regard, Brunel (1999) had functionalized some organic amines onto silica such as piperidine, 1,5,7-triazabicyclo[4.4.0]dec-5-ene and (1*R*,2*S*)-ephedrine. These compounds proved to be efficient base catalysts for transesterification reaction and Knoevenagel¹ condensation. These catalysts are shown in Fig. 1.3.

¹A *Knoevenagel condensation* is a nucleophilic addition of an active hydrogen compound to a carbonyl group followed by a dehydration reaction in which a molecule of water is eliminated. The product is often an alpha, beta conjugated enone.

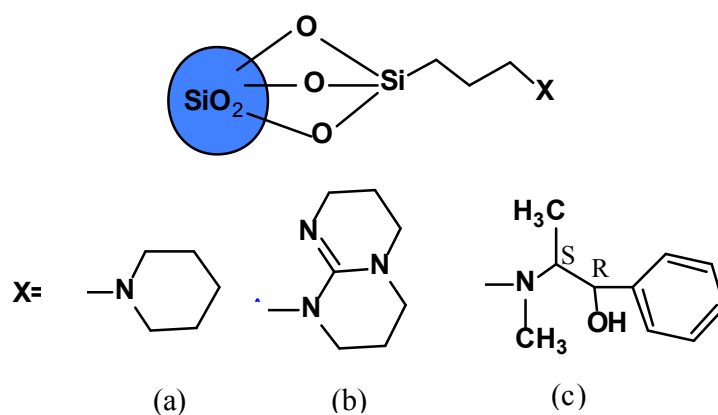


Fig. 1.3: Some examples of base functionalized silica. (a) piperidine, (b) 1,5,7-triazabicyclo[4.4.0]dec-5-ene, (c) (1*R*,2*S*)-ephedrine.

Several pentaalkylguanidines have been prepared and found to be superior catalysts for the preparation of aryl and aryl alkyl ethers from carbonates and for the methylation of phenols with dimethylcarbonate. They also act as effective catalysts for esterification of acids with alkyl chloroformates (Barcelo, et al., 1990).

Kobayashi and Okamoto (2006) investigated the catalytic potential of some organic compounds for acylation of 1-phenylethylalcohol with acetic anhydride (Ac_2O) at room temperature. The investigation showed the catalytic activity of the catalysts followed the sequence as shown in Fig. 1.4. In these studies, these organic molecules were used as homogeneous catalysts.

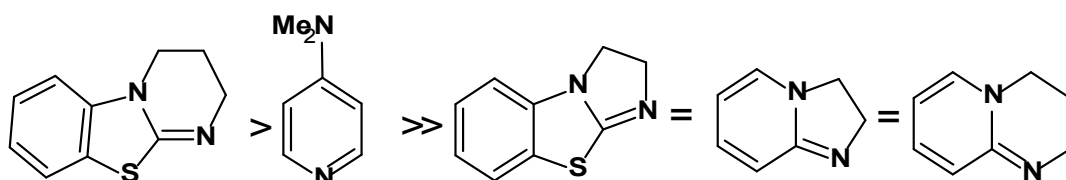


Fig. 1.4: The relative catalytic activity of various organic molecules in the acylation reaction. [adopted from Kobayashi & Okamoto, 2006].

Schuchardt, et al. (1995) explained the use of eight homogenous substituted cyclic and acyclic guanidines on transesterification of rapeseed oil with methanol. The conversion was 90 % yield of methyl esters with in 1 h of reaction. They stated that alkylguanidines can easily be heterogenized on chloromethylated polystyrenes (Schuchardt, et al., 1996). The catalysts that they used showed a good activity towards transesterification.

Kovalchuk et al, (2009) had described the immobilization of heteropolyacids on functionalized silica with (3-propyl-N-pyridinium, 3-propyl-N-methyl and 3-propyl-N-butyl-imidazolium) salts. These catalysts had been used to catalyse the reaction of acetic acid with ethanol. The conversion of acetic acid was measured after 20 h and found to be in the range of 15.5 to 68 %. However, they used multiple techniques for the catalysts preparation and the time used for esterification was quite long with poor yield.

Mercs et al., (2007) had tested ammonium triflates as direct catalysts for esterification reaction using toluene as a solvent in 7 h reaction time at 80 °C. The catalyst had shown good catalytic activity and was easily recovered by simple phase separation.

Rad et al, (2008) had used *N*-(*p*-toluenesulfonyl)imidazole (TsIm) as a catalyst for esterification reaction. In their experiments, the alcohols were refluxed with a mixture of RCO₂Na (R: alkyl and aryl), TsIm, and triethylamine in the presence of catalytic amounts of tetra-*n*-butylammonium iodide (TBAI) in DMF to afford the corresponding esters. Different solvent had been tested and the conversion

of ester was in the range of 0 to 94 % at different reaction times. The maximum conversion of ester was 94 % when DMF was used as the solvent. However, different organic solvents were used during the fabrication process with poor yield of ester.

1.8.2 Esterification by using acid catalyst

Heterocids are widely used in a variety of acid-catalyzed reactions as in esterification. It has been observed that solid acids such as modified forms of zeolites and oxides are very efficient for esterification (Nagaraju & Mehboob,1996). The esterification of glycerol with lauric acid to produce monolaurin using zeolites, sulfonic resins, and sulfonic mesoporous materials as catalysts has been investigated by Bossaert, et al. (1999).

Jackson, et al. (2006) functionalized organosulfonic acid on to mesoporous silica and tested them to see their catalytic performance in the esterification of oleic acid with methanol under supercritical carbon dioxide flow. The study found the activation energy was about 42 kJ mol^{-1} and the activity of the catalyst was shown to be independent of pore size. The catalyst showed higher activity than that of Novozym¹ 435.

¹Novozym 435 is a lipase (lipase B) from *Candida antarctica* produced by submerged fermentation of a genetically modified *Aspergillus* microorganism and adsorbed on a macroporous resin [adapted from Novozym® 435, 2010].

Miao and Shanks (2009) functionalized mesoporous silica with different loadings of propylsulfonic acid groups by using a one-step co-condensation procedure. The resulting materials were effective in the esterification of acetic acid with methanol. They used this as a model reaction for stabilization of bio-oil. The catalyst showed multiple cycle stability without significant loss of activity.

Yang, et al. (2005) described the synthesis of sulfonic acid-functionalized hydrophobic mesoporous benzene-silica with lamellar pore wall structure. They found that the mesoporous benzene-silica was attached to propylsulfonic groups to the crystal-like periodic pore walls. The catalyst showed higher conversion compared to the commercial Nafion-H (sulfonated tetrafluoroethylene, $C_7HF_{13}O_5S.C_2F_4$).

1.9 Esterification of long-alkyl chain fatty acid

Esterification of long-alkyl chain fatty acids with alcohols represents a well-known category of liquid-phase reactions of considerable industrial interest due to the enormous practical importance of organic ester products (Altıokka & Çıtak, 2003). Recently, the esterification of long-alkyl chain fatty acids has spurred a great deal of interest due to their important and multiple applications. For example, long-alkyl chain fatty acid esters can be used as a biofuel. The esters produced from long-alkyl chain fatty acids (12–20 carbon atoms) and short-alkyl chain alcohols (three to eight carbon atoms) have been used increasingly in the food, detergent, cosmetic and pharmaceutical industries (Bauer, et al., 1990). Esters prepared from the reaction of long-alkyl chain acids with long-chain alcohols (12–20 carbon atoms) also have important applications as plasticisers and lubricants (Gandhi, et al., 1995). It is

economically important to develop catalysts for the production of such esters from cheaper and more broadly available raw materials.

1.10 Objectives of the study

As mentioned earlier, scientists discovered silanol groups on silica surface in 1930. These silanol groups have been used to heterogenize silylating agents through heterogeneous methods. Due to the unfavourable conditions of the current method, this study aims to improve on these conditions. It must be clarify that Sac and Mela have never been used as a homogenous or heterogeneous catalyst in any form based on the literature reviewed. The main objectives of this work are:

1. To modify the silica extracted from RHA with different silylating agents such as CPTES, MPTMS and APTES via a simple one-pot synthesis.
2. To use this new method to synthesize RHAC-Sac, RHAPrMela and RHAPrSO₃H as heterogeneous catalysts.
3. To characterize the catalysts using various spectroscopic and microscopic techniques such as CHN analysis, TGA, Powder X-ray, N₂ adsorption-desorption, FT-IR, ²⁹Si and ¹³C MAS NMR, SEM/EDX and TEM.
4. To investigate the catalytic potential of the catalysts on the esterification of different alcohols with acetic acids.
5. To determine the reaction kinetic parameters of each catalyst in the esterification reaction.

1.11 Outline of Thesis

This thesis consists of six chapters. They are briefly outlined below.

Chapter 1 provides an overview on the study and reviews the available literature on silica modification. It describes the synthesis strategies and the mechanism of synthesis. It also discusses some relevant materials such as Sac, Mela, acid and base catalysts for esterification.

Chapter 2 gives an account of the synthesis of silica with silylating agent using a simple strategy and also describes the catalysts synthesis with physicochemical characterization method used in this study. It also describes the experimental procedures used in this study.

Chapter 3 and 4 deals with the physicochemical characterization of the samples synthesized by different methods. The elemental composition was determined using a combination of chemical analysis (CHN) with Energy Dispersive X-ray (EDX). Thermal analysis and N₂-sorption studies are used to calculate the loading of the grafted organic molecule. FT-IR spectroscopy is used to monitor the change in the functional groups. Solid state ²⁹Si and ¹³C MAS NMR studies were carried out to understand the catalysts structures. X-ray diffraction (XRD), Transmission Electron Microscopy (TEM) and Scanning Electron Microscopy (SEM) were also used to determine the morphology of the modified silica and the synthesised catalysts.

Chapters 5 describe the catalytic performances of the bases and acid catalyst samples. The esterification of ethanoic acid versus different alcohols were investigated. The effect of reaction time, temperature, molar ratio of the reactants and the amount of the catalyst on esters formation were evaluated to optimize the reaction conditions. The reusability of the catalyst, the temperature effect on the regeneration of the catalyst, the reactions of methanol with different acids (acetic acid (C2), capric acid (C10) and myristic acid (C14)), reaction kinetics and mechanisms are also reported.

Finally, in **Chapter 6** a summary of the results obtained and the conclusions are presented.

Chapter Two

Experimental Methods

2.0 Raw materials

All chemicals are of AR grade or high purity and was used directly without further purification. These include; sodium hydroxide (System, 99%), nitric acid (System, 65%), CPTES (Sigma–Aldrich, 95%), MPTMS (Merck, 95%), APTES (Merck, 98%), toluene (J.T. Baker, 99.8%), Sac (Fluka, 99%), Mela (Acros Organics, 99%), hydrogen peroxide (J.T. Baker, 30%), triethylamine (Et₃N) (R&M chemical, 99%), dimethylformamide (DMF) (System, 99.5%), dichloromethane (DCM) (Merck, 99%), methanol (System, 99.9%), ethanol absolute (HmbG Chemical, 99.74%), 1–propanol & 1–butanol (R&M chemical, 99.5%), benzyl alcohol (Unilab, 97%), tertiary–butyl alcohol (Merck, 99%), 2–propanol (Unvasol, 99%), acetic acid (System, 99.5%), capric acid (C10) (Acidchem, 99%), myristic acid (C14) (Acidchem, 98%), and n–decane (Acros Organics, 99%). The rice husk (RH) was collected from a rice mill in Penang, Malaysia.

2.1 Extraction of silica from rice husk

The rice husk RH was chosen as the source of amorphous silica as it was available in abundance. The silica was extracted from RH according to a reported method Kalapathy, et al. (2000); Ahmed (2008).

The RH was washed with water then rinsed with distilled water and dried at room temperature for 24 h. A 35 g sample of the cleaned RH was stirred with